

Results from the Pierre Auger Observatory: Mass Composition of Ultra-high Energy Cosmic Rays and proton-air cross-section at $\sqrt{s} = 57$ TeV

G. Cataldi², G. Cocciolo^{2,3}, M. R. Coluccia^{1,2}, S. D'Amico^{2,3}, I. De Mitri^{1,2}, U. Giaccari^{1,2,5}, G. Marsella^{1,2}, D. Martello^{1,2}, L. Perrone^{1,2}, M. Settimo^{1,2,4} and the Pierre Auger Collaboration

¹ Dipartimento di Matematica e Fisica “Ennio De Giorgi”, Università del Salento, Italy

² Istituto Nazionale di Fisica Nucleare sez. di Lecce, Italy

³ Dipartimento di Ingegneria dell'Innovazione Università del Salento, Italy

⁴ now at the Dept. of Physics, University of Siegen, Germany

⁵ now at Universidade Federal do Rio de Janeiro (UFRJ)

1. Introduction

The Pierre Auger Observatory started collecting data in 2004 [1–3]. The Observatory uses hybrid measurements of air showers recorded by an array of 1660 water Cherenkov surface stations covering an area of 3000 km², together with 24 air fluorescence telescopes that observe the development of air showers in the atmosphere above the array during dark nights.

An infill array [4] with half the grid size has been completed and is currently taking data with a threshold of about $3 \cdot 10^{17}$ eV. Moreover, three high-elevation telescopes (HEAT) [5] have begun operation and, together with the infill array in the FOV of the telescopes, will allow us to extend the hybrid measurements further down to 10^{17} eV thus covering with full efficiency the region of the transition from galactic to extra-galactic cosmic rays. The deployment of buried muon detectors (AMIGA) [6] in the infill area is in progress and an extensive R&D program for radio and microwave detection of UHE air showers is under way. The construction of the Auger Engineering Radio Array (AERA) has started [7] and several GHz-antennas are installed and taking data [8].

These extensions and new technologies may enhance the performance and capabilities of the Auger Observatory in Argentina and, in parallel, will explore their potential for a future much larger ground based observatory.

2. Mass Composition

The measurement of the cosmic ray flux has to be complemented by an independent measurement of primary mass composition, with the goal of separating the different scenarios of origin and propagation of cosmic rays.

The composition can be obtained from mea-

surements of various shower observables, primarily the atmospheric depth at which the shower reaches its maximum size, X_{\max} .

As the fluorescence telescopes can directly observe the shower longitudinal profile, hybrid events are used for this analysis. The position of X_{\max} is derived from a fit to a Gaisser-Hillas function. Only events with a precise reconstruction of the geometry and of the longitudinal profile are selected. The X_{\max} has to be observed in the FD field of view and quality cuts on the aerosol content and cloud coverage are applied. To avoid mass-dependent biases due to the limited field of view of the FD, the analysis is restricted to a geometrical volume that equalizes the selection efficiency over the major part of the parent X_{\max} distribution [9,10].

Hybrid data collected between December 2004 and September 2010 have been used and 6744 events (with $E \geq 10^{18}$ eV) fulfill the selection criteria. In Fig. 1 $\langle X_{\max} \rangle$ and its RMS are shown as a function of energy [10]. Both show a characteristic change at $E \simeq 5 \cdot 10^{18}$ eV indicating an increasingly heavier composition when compared to air shower simulations. The X_{\max} resolution is found to be about 20 g cm^{-2} [9] after detailed simulations of the detector and several cross-checks with events observed by two or more FD sites.

As mentioned in the previous section, the systematic uncertainty on the energy scale is about 22%. The total systematic uncertainty on $\langle X_{\max} \rangle$ ranges between 10 g cm^{-2} at low energy and 13 g cm^{-2} at high energy. It includes contributions from the uncertainties in the calibration, the atmospheric data, the reconstruction and the event selection. The systematic uncertainty on $\text{RMS}(X_{\max})$ has been quoted as 5 g cm^{-2} .

A detailed comparison of Auger results with other experiments, namely HiRes, Telescope Ar-

ray and Yakutsk, has been shown in [11].

Although the SD cannot directly observe the X_{\max} , several observables (e.g. muon content, muon production depth, azimuthal asymmetry of the signal rise time) are related to the mass of the primary particle and to the shower development. The mass sensitive observables from SD can provide complementary information, with independent statistical uncertainties. The higher statistics allow us to extend this measurement to higher energies than possible with the FD. Details and a comparison between the resulting composition from SD and FD-based measurements are given in [10].

The position of the shower maximum is also influenced by the depth of the first interaction, i.e. by the cross-section of the primary particle with air. As a consequence, the interpretation of shower observables in terms of primary mass suffers from the lack of knowledge of interactions properties at the highest energies, propagating into air shower simulations. The next section will summarize the status of cross-section measurement carried out with the Pierre Auger Observatory.

3. The proton-air cross-section

Auger hybrid data provide a tool to investigate the matter interaction properties at energies well above the upper limits achievable with the accelerators nowadays available.

The tail of the X_{\max} distribution is sensitive to the proton-air cross-section, a fact exploited in the pioneering work of the Fly's Eye Collaboration [12]. For this purpose, the shape of the distribution of the largest values of X_{\max} is analyzed for a sample of hybrid events. The tail of X_{\max} distribution that contains the 20% of deepest showers exhibits the expected exponential shape $dN/dX_{\max} \propto \exp(X_{\max}/\Lambda_f)$, see Fig. 2. It is directly related to the p-air cross-section via $\sigma_{p-air} \propto 1/\Lambda_f$.

In practice, to properly account for shower fluctuations and detector effects, the exponential tail is compared to Monte Carlo predictions. Any disagreement between data and predictions is then attributed to a modified value of the proton-air cross-section [14]. In this analysis, the energy interval is restricted between 10^{18} and $10^{18.5}$ eV which corresponds to a center-of-mass energy in the nucleon-nucleon system of $\sqrt{s} = 57$ TeV. This interval has been chosen because of high statistics in the data and because of the composition being compatible with a dominance of protons (see. Sec. 2).

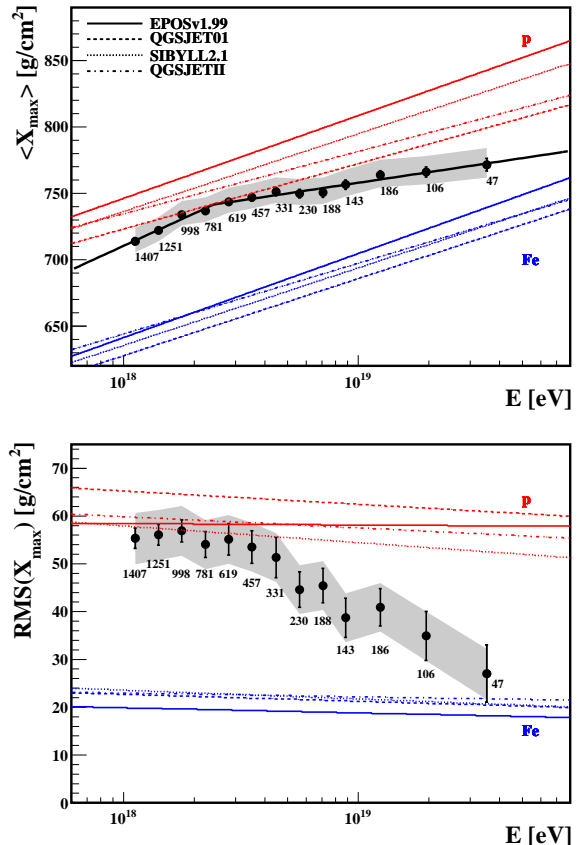


Figure 1. $\langle X_{\max} \rangle$ and $\text{RMS}(X_{\max})$ as a function of energy compared with air shower simulations using different hadronic interaction models [10].

A possible contamination of He primaries could mimic a larger cross-section (e.g. by 20 mb for 20% He contamination) while a photon contamination could reduce the cross-section by at most 10 mb.

Combining the results one finds

$$\sigma_{p-air} = [505 \pm 22(\text{stat})_{-36}^{+28}(\text{syst})] \text{ mb}$$

at a center-of-mass energy of 57 ± 6 TeV. This result is shown in comparison to other data and models in Fig.3. The result favors a moderately slow rise of the cross-section towards higher energies, well in line with recent results from LHC [13].

A conversion of the derived σ_{p-air} measurement into the more fundamental cross-section of proton-proton collisions using the Glauber framework is given in [14].

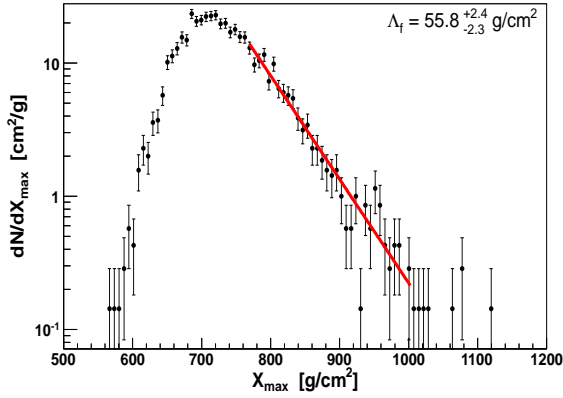


Figure 2. Unbinned likelihood fit to obtain Λ_f (thick line).

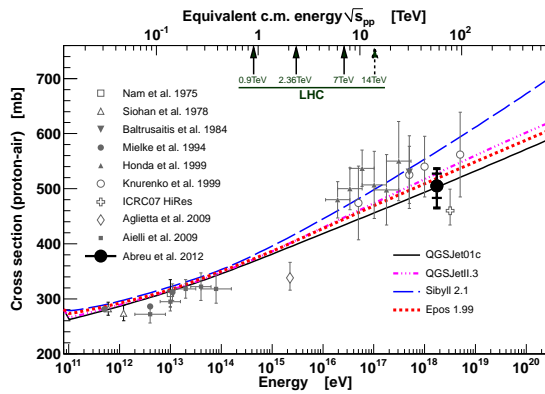


Figure 3. Proton-air cross-section compared to other measurements and model predictions (for references see [14]). The inner error bars are statistical only, while the outer include all systematic uncertainties for a helium fraction of 25% and 10 mb photon systematics.

REFERENCES

1. The Pierre Auger Collaboration, Nucl. Instrum. Meth. **A 523** (2004) 50.
2. The Pierre Auger Collaboration, Nucl. Instrum. Meth. **A 620** (2010) 227.
3. I. Allekotte et al. for the Pierre Auger Collaboration, Nucl. Instrum. Meth. **A 586** (2008) 409.
4. I. Mariş for the Pierre Auger Collaboration, Proc. 32nd ICRC, Beijing, China (2011), arXiv:1107.4809.

5. H-J. Mathes, for the Pierre Auger Collaboration, Proc. 32nd ICRC, Beijing, China (2011), arXiv:1107.4807.
6. F. Sanchez, for the Pierre Auger Collaboration, Proc. 32nd ICRC, Beijing, China (2011), arXiv:1107.4807.
7. The Pierre Auger Collaboration, JINST **7** (2012) P11023.
8. P. Facal for the Pierre Auger Collaboration, UHECR-2012, CERN, February 13rd-17th, (2012).
9. The Pierre Auger Collaboration, Phys. Rev. Lett. **104** (2010), 091101.
10. P. Facal, for the Pierre Auger Collaboration, Proc. 32nd ICRC, Beijing, China (2011), arXiv:1107.4804.
11. E. Barcikowski, J. Bellido, J. Belz, Y. Egorov, S. Knurenko, V. de Souza, Y. Tsunesada, and M. Unger for the HiRes, Pierre Auger, Telescope Array and Yakutsk Collaborations, UHECR-2012, CERN February 13rd-17th, (2012).
12. R. Ellsworth et al., Phys. Rev. D **26**, (1982) 336, R. Baltrusaitis et al., Phys. Rev. Lett. **52**, (1984) 1380.
13. TOTEM Collaboration, Europhys. Lett. **96**, (2011) 21002; ATLAS Collaboration, Nature Commun. **2** (2011) 463; CMS Collaboration, arXiv:1205.3142v1.
14. The Pierre Auger Collaboration, Phys. Rev. Lett. **109** (2012) 062002.